AIAA JOURNAL
Vol. 48, No. 3, March 2010

Analytical Modeling of Cracked Thin-Walled Beams Under Torsion

Thi D. Dang,* Rakesh K. Kapania,† and Mayuresh J. Patil‡
Virginia Polytechnic Institute and State University, Blacksburg, Virginia 24061-0203

DOI: 10.2514/1.45393

We present an analytical model, derived using the principle of virtual work, for closed and open thin-walled beams subjected to torsion. Nonclassical effects like primary and secondary torsional warping are taken into account. A closed-form expression for mode II stress-intensity factor for thin-walled beams with a longitudinal crack is derived. We start by finding analytical solutions based on Vlasov's torsional beam theory for thin-walled beams with any cross sections. We then use the calculated stress of a rectangular thin-walled beam to determine an analytical expression for mode II stress-intensity factor. Finally, we add a correction factor to account for complex behavior of long cracks. Examples are presented to illustrate the effectiveness of the current model, and it is validated by comparison with detailed finite element results obtained using ABAQUS.

I. Introduction

THIN-WALLED structures are widely used in practical applications in structural engineering such as marine, automobile, aerospace, nuclear power plant, and civil engineering. The presence of cracks and other flaws in such structures is a quite common situation. Thin-walled sections are composed of very slender plates with the presence of cracks and have complex modes of failure and deformation. The stresses and failure modes in thin-walled sections can be quite difficult to predict (Papangelis and Hancock [1]). Therefore, the understanding of the behavior of thin-walled structures under different loadings is a very important problem. For example, in ship structures, complicated torsional loading on the hull of modern containership determines the structural design of the ship hull. Also, in aerospace engineering, wings are among the most critical structural units of an airplane and their load-bearing capability determines, to a great extent, the aircraft's safety in flight. Multi-axial dynamic loadings acting on an airplane during a flight may lead to the onset and growth of fatigue cracks in wings and other structures.

The present paper deals with thin-walled beams; specifically, we consider a beamlike wing box under torsion, for which the thin-walled cross sections warp when torsional loads act on it. The wing box is initially assumed to have a rectangular, closed cross section. A discrete source damage, modeled as a crack along the span of the beam, makes the wing an open section beam locally. The study of the behavior of cracked beams was carried out by many authors during the last two decades. Kapania and Castel [2] proposed a model using one-dimensional finite elements for aeroelastic analysis of undamaged and damaged wings. The formulation takes into account the effect of transverse shear and the bending-stretching couplings. The modal analysis of cracked beams has been performed by many others (Dimarogonas [3], Ruotolo and Surace [4], Chondros et al. [5], Song et al. [6], Wang et al. [7], and Wang and Inman [8]), but all of these authors worked on solid beams with transverse cracks, and most of the cases are related to cracked beams under bending loads alone.

The existence of cracks or defects in thin-walled structures is inevitable and can cause unexpected failure. One of the most important parameters in fracture mechanics is the stress-intensity factor (SIF), which represents intensification of the stress field in the vicinity of the crack tip. Therefore, an estimate of the stress-intensity factors is an interesting and important problem and has attracted much attention. Analytical or experimental expressions for SIFs were derived by many researchers for simple crack configurations and have been reported in literature (Sih [9]). Newman and Raju [10,11] published a series of papers on empirical equations of SIFs, which were obtained by fitting equations to finite element results. For cylindrical shells, Folias [12] derived a closed-form expression for the mode I stress-intensity factor of a longitudinal crack in a pressurized cylindrical shell using a correction factor called the Folias correction (Janssen et al. [13]). Stress-intensity factors of cylindrical shells under bending and tension were also studied by Sanders [14,15].

For cracked-beam problems, Herrmann and Sosa [16] used an elementary beam theory to estimate the strain energy rate as the crack is widened into a fracture band. The strain energy rate is used to study cylindrical bars with cracks in the presence of tension. Bazant [17] improved Herrmann and Sosa's [16] work by suggesting an additional correction factor obtained by matching with an analytical solution. The theory of Herrmann and Sosa was also used for some simple crack configurations (Gao and Herrmann [18] and Muller et al. [19]), in which they improved the approximation by a correction factor that can be obtained by matching with asymptotic solutions. The methods of Bazant [17], Herrmann and Sosa [16], Gao and Herrmann [18], and Muller et al. [19] are not feasible when the geometry or loadings are complicated and asymptotic solutions do not exist, as is the case in our problem. Based on Herrmann and Sosa's [16] work, Dunn et al. [20] derived a closed-form expression for the stress-intensity factors for a cracked I-beam subjected to a bending moment using a correction factor that was obtained by fitting data obtained using detailed finite element solutions. Xie et al. [21,22] used Herrmann and Sosa's [16] theory to propose the concept of the crack-mouth-widening energy-release rate G^* to estimate SIFs of some crack configurations such as cracked solid beams under bending and cracked cylinder under torsion or bending. However, the expressions derived by their approach (Xie et al. [21,22]) for SIFs look rather complex and are not convenient for use in design. All of the authors mentioned above worked on beams with a transverse crack, and most of them estimated stress-intensity factors for cracked solid beam with rectangular cross sections. Recently, Xie et al. [23] derived analytical solutions using the crack-mouth-widening

Presented as Paper 2367 at the 50th AIAA/ASME/ASCE/AHS/ASC Structures, Structural Dynamics, and Materials Conference, Palm Springs, CA, 4–7 May 2009; received 11 May 2009; revision received 23 October 2009; accepted for publication 3 November 2009.

*Postdoctoral Fellow, Department of Aerospace and Ocean Engineering; ddthi@vt.edu. Member AIAA.

†Mitchell Professor, Department of Aerospace and Ocean Engineering; rkapania@vt.edu. Associate Fellow AIAA.

‡Assistant Professor, Department of Aerospace and Ocean Engineering; mpatil@vt.edu. Senior Member AIAA.

energy-release rate G^* for SIFs of cracked thin-walled tubes with rectangular cross sections under tension and bending, and with transverse cracks of elliptical or square shapes. Numerical methods (e.g., thin-shell finite element models) are widely used for analysis and computation of thin-walled structures (Yang et al. [24]), but the computational cost of the analysis is expensive. This is especially true for modeling of cracked thin-walled structures. To get the accurate stress-intensity factors or to predict crack path by numerical methods, one has to calculate the crack tip stress/strain field accurately. The essential requirements for the numerical methods are to resolve the stress field around the crack tip and to track the crack path. These requirements will challenge traditional finite element methods and the results greatly depend on a user's experience.

In this paper, we develop an analytical model for thin-walled rectangular beams under torsion in which the nonclassical effects like primary and secondary torsional warping are taken into account. The governing equations and associated boundary conditions are derived using the principle of virtual work. The stress, displacement fields, and twist angles are computed for closed thin-walled beams and for open thin-walled beams. We derive a closed-form expression of the mode II stress-intensity factors for the thin-walled beams under torsion with a small crack along the beam span. An additional correction factor in the form of a simple expression is obtained based on a calibration using shell finite element calculations for a long crack, and this formula can be used to rapidly obtain the mode II stress-intensity factor.

The paper is organized as follows. In Sec. II, an analytical model is presented, in which analytical solutions for closed and open beams with rectangular cross sections subjected to pure torsion are given. Closed-form expressions for the mode II stress-intensity factor for thin-walled beams with a longitudinal crack are derived for the first time. Numerical examples and validations are presented in Sec. III. Summary and conclusions are summarized in Sec. IV.

II. Analytical Model

Consider a thin-walled structure: for example, a beam with a with uniform rectangular cross section, as shown in Fig. 1. Let t be its wall thickness. In general, t can be varying along the midline of the cross-sectional contour $t = t(s)$ (see Fig. 2); b and h are dimensions of the cross section (b is the width of the beam, h is the height of the beam); and L is the length of the beam. Let $t_{\max}$ denote the maximum wall thickness. According to Librescu and Song [25], a structure is defined as a thin-walled structure if

$$\frac{t_{\max}}{\min(b,h)} \leq 0.1 \qquad \frac{\max(b,h)}{L} \leq 0.1 \tag{1}$$

A thin-walled section is said to be closed/open when the locus of points defining the centerline of the wall forms a closed/open contour. Figure 1 illustrates an example for a closed section.

A. Analytical Solutions for Thin-Walled Beams with Arbitrary Cross Section Under Torsion

We consider a thin-walled beam under pure torsion T at its tip and the distributed-applied twist moment along the beam span m_x. The beam has arbitrary cross section with longitudinal axis x and principal axes y and z with origin O. The point P is the center of twist of the cross section, and the point C is the origin of the contour coordinate. At any point A on the middle surface of the thin-walled section, we define a local coordinate system (x, s, n) with unit vectors $\mathbf{i}$, $\mathbf{j}$, and $\mathbf{k}$, respectively (see Fig. 2).

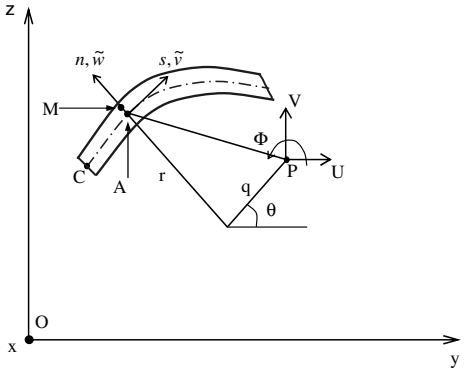

Fig. 2 Coordinates for an open cross section.

We have the following vectors:

$$\begin{aligned} \mathbf{PA} &= \mathbf{q} + \mathbf{r} = q\mathbf{j} + r\mathbf{k} \\ \mathbf{PM} &= \mathbf{PA} + \mathbf{AM} = q\mathbf{j} + (r+n)\mathbf{k} \end{aligned} \tag{2}$$

where r is the perpendicular distance from the shear center to the tangent to the centerline of the cross section, and q is the perpendicular distance from the shear center to the normal to the centerline.

The classical Saint-Venant torsion theory (Todhunter and Pearson [26]), which is the basis for present-day analysis of rods under torsion, proved that under torsion, a transverse noncircular planar section does not remain plane. The original plane cross-sectional surface becomes a warped surface. In Saint-Venant torsion theory, the cross section is assumed to warp freely out of its plane and the rate of twist of the cross section $\beta'(x)$ is assumed to be constant. This leads to some errors in the case of nonuniform torsion, where the rate of twist $\beta'(x)$ varies along the length of the beam. The warping axial displacement in Vlasov's general torsion theory (Gjelsvik [27] and Murray [28]) is defined as

$$u = \beta'(x)\psi(s,n) \tag{3}$$

where $\psi(s,n)$ is the warping function, and $\beta'(x)$ is the derivative of $\beta(x)$ with respect to x. This equation is valid for both the open and closed section tubes provided that $\psi(s,n)$ is correctly computed for open and closed sections.

We consider the displacement field at a point $M(x,s,n)$ in the cross section:

$$\mathbf{u}_M(x,s,n) = \beta(x)\mathbf{i} \times \mathbf{PM} + \beta'(x)\psi(s,n)\mathbf{i} \tag{4}$$

where $\times$ is the cross product of two vectors $\mathbf{i}$ and $\mathbf{PM}$. If u, $\tilde{v}$, and $\tilde{w}$ are the components of u_M in the x, s, and n directions, we obtain the following displacement field from Eq. (4):

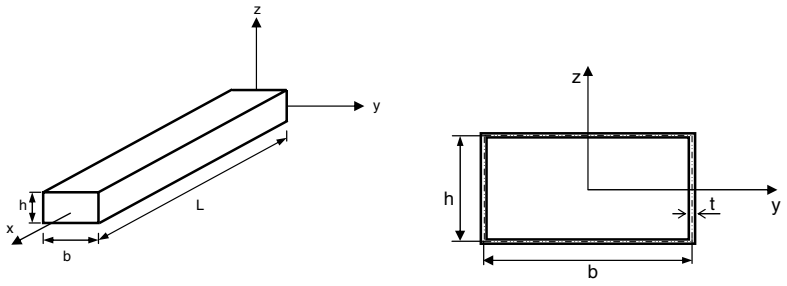

Fig. 1 An example of the thin-walled beam configuration and coordinates.

$$u(x,s,n) = \beta'(x)\psi(s,n)$$
$$\tilde{v}(x,s,n) = -[r(s)+n]\beta(x)$$
$$\tilde{w}(x,s,n) = q(s)\beta(x) \tag{5}$$

The strain field for the cross-sectional beam is computed from Eq. (5) as

$$\varepsilon_{xx} = \beta''(x)\psi(s,n)$$
$$\gamma_{xs} = \beta'(x)\left[\frac{\partial\psi(s,n)}{\partial s} - (r+n)\right]$$
$$\gamma_{xn} = \beta'(x)\left(\frac{\partial\psi(s,n)}{\partial n} + q\right) \tag{6}$$

The stress field is obtained from the stress/strain relation as

$$\sigma_{xx} = E\cdot\beta''(x)\cdot\psi(s,n)$$
$$\sigma_{xs} = G\cdot\beta'(x)\cdot\left[\frac{\partial\psi(s,n)}{\partial s} - (r+n)\right] \tag{7}$$
$$\sigma_{xn} = G\cdot\beta'(x)\cdot\left(\frac{\partial\psi(s,n)}{\partial n} + q\right)$$

where E is the elastic modulus and G is the shear modulus of the material.

We can derive the governing equations and associated boundary conditions from the principle of virtual work as

$$\delta\pi(\delta\beta) = \delta U + \delta V = 0 \quad \forall\ \delta\beta \tag{8}$$

where $\delta\beta$ is the kinematically admissible generalized virtual displacement.

The variation of the strain energy is given as

$$\delta U = \int_\Omega \boldsymbol{\sigma}\delta\boldsymbol{\varepsilon}\,\mathrm{d}\Omega = \int_\Omega (\sigma_{xx}\delta\varepsilon_{xx} + \sigma_{xn}\delta\gamma_{xn} + \sigma_{xs}\delta\gamma_{xs})\,\mathrm{d}\Omega \tag{9}$$

Substituting Eqs. (6) and (7) into Eq. (9), the variation of strain energy becomes

$$\delta U(\delta\beta) = \int_\Omega \left\{E\psi^2\beta''\delta\beta'' + G\beta'\left[\left(\frac{\partial\psi}{\partial n} + q\right)^2 + \left(\frac{\partial\psi}{\partial s} - (r+n)\right)^2\right]\delta\beta'\right\}\mathrm{d}\Omega \tag{10}$$

where Ω is the volume of the beam. Let us define

$$k_1 = \int_A E\cdot\psi^2\,\mathrm{d}A$$
$$k_2 = \int_A G\cdot\left\{\left(\frac{\partial\psi}{\partial n} + q\right)^2 + \left[\frac{\partial\psi}{\partial s} - (r+n)\right]^2\right\}\mathrm{d}A \tag{11}$$

where A is the area of the beam cross section. Taking integrations given in Eq. (10) by parts, we obtain

$$\delta U = k_1\beta''\delta\beta'|_0^L - k_1\beta'''\delta\beta|_0^L + k_2\beta'\delta\beta|_0^L + \int_0^L (k_1\beta'''' - k_2\beta'')\delta\beta\,\mathrm{d}x \tag{12}$$

The variation of the potential of the applied loads (here, the pure torsion) is stated as

$$\delta V(\delta\beta) = -\int_0^L m_x\delta\beta\,\mathrm{d}x - T\delta\beta|_L \tag{13}$$

where m_x is the distributed applied torque.

Substituting Eqs. (12) and (13) into Eq. (8), we finally obtain

$$\delta\pi = k_1\beta''\delta\beta'|_0^L - k_1\beta'''\delta\beta|_0^L + k_2\beta'\delta\beta|_0^L + \int_0^L (k_1\beta'''' - k_2\beta'' - m_x)\delta\beta\,\mathrm{d}x - T\delta\beta|_L = 0 \quad \forall\ \delta\beta \tag{14}$$

The governing equation is derived as

$$k_1\beta'''' - k_2\beta'' - m_x = 0 \tag{15}$$

The associated boundary conditions for the thin-walled beam under pure torsion with one end clamped are derived as

$$\begin{cases} (-k_1\beta''' + k_2\beta' - T)|_L = 0 \\ \beta''|_L = 0 \\ \beta|_0 = 0 \\ \beta'|_0 = 0 \end{cases} \tag{16}$$

Assume that the beam is under a tip torque only: thus, $m_x = 0$. Solving the boundary-value-problem equations (15) and (16), we can obtain the closed-form expression of the twist angle for the thin-walled beams:

$$\beta = \frac{T}{k_2}\left[\frac{\tanh(\lambda L)}{\lambda}\cosh(\lambda x) - \frac{\sinh(\lambda x)}{\lambda} + x - \frac{\tanh(\lambda L)}{\lambda}\right] \tag{17}$$

where

$$\lambda = \sqrt{\frac{k_2}{k_1}} \tag{18}$$

The form of the exact solution in Eq. (17) is the same as the one in Oden and Ripperger [29] and Fatmi [30] for rectangular thin-walled beams; however, k_1 and k_2 are computed for any cross sections.

B. Warping Function

1. *Warping Function for Rectangular Box Beams*

The warping function for rectangular box beams (see Fig. 1) is taken in the form (Smith and Chopra [31]) of

$$\psi(y,z) = \zeta yz \tag{19}$$

where ζ and α are given as

$$\zeta = -\frac{(1-\alpha)}{(1+\alpha)} \quad \text{and} \quad \alpha = \left(\frac{b}{h}\right)\left(\frac{t_v}{t_h}\right)\left(\frac{G_v}{G_h}\right) \tag{20}$$

where G_h and G_v are effective in-plane shear stiffness for each horizontal and vertical wall, respectively.

For uniform wall thickness of the cross section and isotropic material, we have

$$\zeta = \frac{b-h}{b+h} \tag{21}$$

where b is the width of the beam, and h is the depth of the beam.

For example, we consider a closed cross section of thin-walled beam with $b = 0.4$, $h = 0.2$, and $t = 0.01$, the contour warping function, for a rectangular cross section, as shown in Fig. 3. In the case of the rectangular thin-walled beam with the uniform wall thickness of the cross section, the shear center is identical to the centroid of the cross section.

A generic procedure to determine the warping function for closed cross sections of thin-walled beams is shown in the Appendix.

2. *Warping Function for Cracked-Beam Cross Sections*

At the cracked section, we consider its cross section as an open cross section. When a thin-walled member is twisted, points on the cross section move parallel to the longitudinal x axis. This phenomenon is called warping; the warping displacement u at a point in the cross section in Vlasov's beam theory (Gjelsvik [27] and Murray

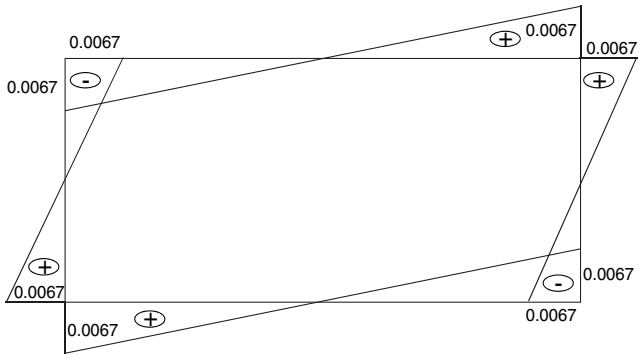

Fig. 3 Contour warping function for rectangular thin-walled beams.

[28]) is defined in Eq. (3). The warping deformation is composed of the warping of the contour and the warping of the thickness, and the warping function is defined by

$$\psi = \int_{C(s)} r(s)\,\mathrm{d}s - nq(s) \tag{22}$$

The first term on the right-hand side of Eq. (22) is called the contour warping function and the second is the thickness warping function. This second term has little effect on the torsional properties of a thin beam and, most frequently, is neglected when analyzing thin-walled beams for most practical applications (Prokic [32]). For example, for the heaviest commercially available I beams, the maximum thickness contribution to the warping displacement is about 5% (Gjelsvik [27]). In this study, we consider both terms in Eq. (22).

In Eq. (22), $C(s)$ is the segment of the contour lying between the origin and an arbitrary point, and $r(s)$ is the perpendicular distance from the shear center to the tangent to the centerline of the cross section of an element ds located a distance s along the centerline of the cross section; similarly, $q(s)$ is the perpendicular distance from the shear center to the normal to the centerline (see Fig. 2).

To determine the warping function, we follow the procedure described by Murray [28]. A brief description of this procedure is shown in the Appendix.

We consider a thin-walled beam with a crack located along the span of the beam in the plane xoz. We will have an open cross section at the cracked domain. The beam has dimensions $b = 0.4$, $h = 0.2$, and $t = 0.01$, as shown in Fig. 4.

Following the procedure in the Appendix, the location of the shear center of the cross section is $x = 0$ and $y = -0.24$, and the warping function is as shown in Fig. 5.

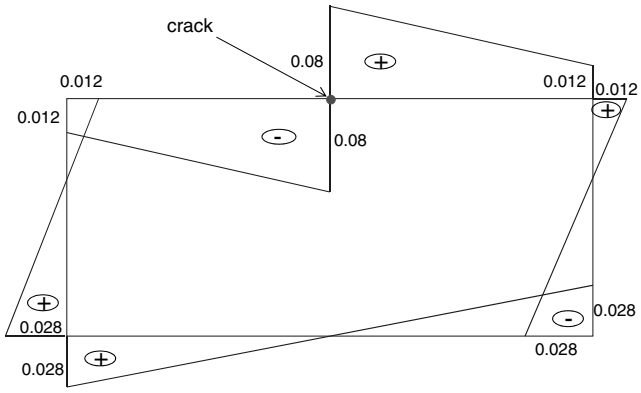

Fig. 5 Contour warping function for cracked cross-section thin-walled beams.

C. Closed-Form Expression of Stress Intensity Factors for Longitudinally Cracked Thin-Walled Beams

We consider a cracked thin-walled beam, as shown in Fig. 6. The beam before damage has a uniform. rectangular, closed cross section. We assume that an initial crack located at middle of the beam in the xoz plane along the span of the beam with the crack length $2a$. The length of the beam is L, the width of the beam is b, and the height of the beam is h. A torsional loading T is applied at the tip of the beam.

In the case of the rectangular thin-walled beam with the uniform wall thickness of the cross section, the shear center is identical to the centroid of the cross section, and the notations s and n are replaced by z and y, respectively. For an isotropic rectangular thin-walled beam under a tip torque, shear stresses at the top surface of the beam are computed from Eqs. (7) and (19) as

$$\sigma_{xy} = G \cdot \beta' \cdot \left[\frac{\partial \psi(y,z)}{\partial y} + z\right] \tag{23}$$

From Eq. (17) we have the derivative of the twist angle as

$$\beta' = \frac{T}{k_2}[\tanh(\lambda L)\sinh(\lambda x) - \cosh(\lambda x) + 1] \tag{24}$$

Taking into account Eqs. (19–21) and (24), we can rewrite Eq. (23) in the form

$$\sigma_{xy} = G \cdot \frac{bh}{(b+h)} \cdot \frac{T}{k_2} \cdot [\tanh(\lambda L)\sinh(\lambda x) - \cosh(\lambda x) + 1] \tag{25}$$

For an isotropic rectangular thin-walled beam, the stiffness coefficient k_2 from Eq. (11) can be computed as

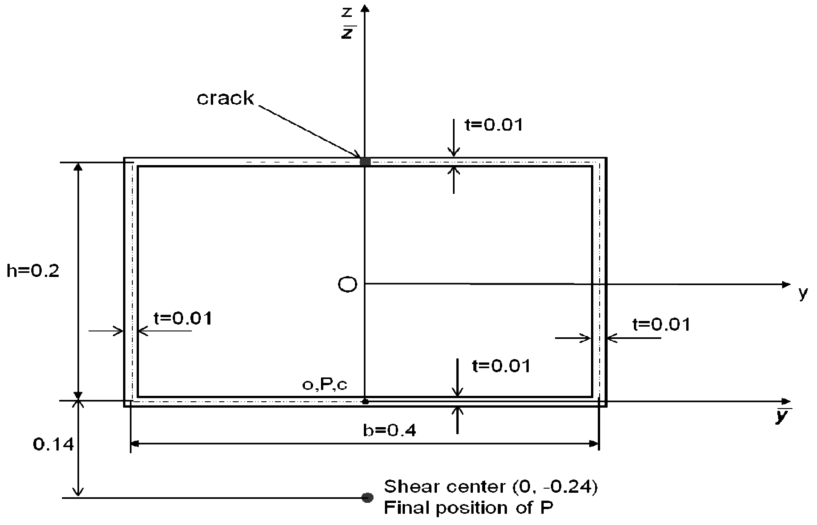

Fig. 4 Coordinate system $\bar{x}o\bar{y}$, the pole P, the starting point O, and dimensions of the open cross section.

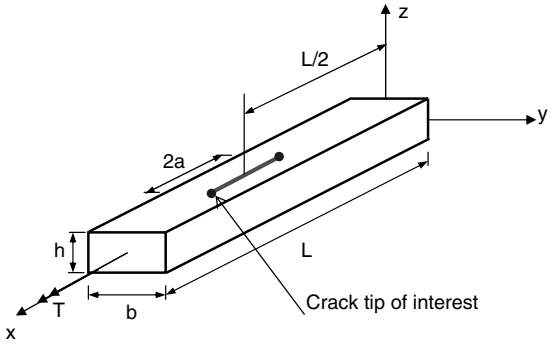

Fig. 6 Cracked-beam scheme under tip torque.

$$k_2 = G \cdot J = \frac{G \cdot 2 \cdot (b \cdot h)^2 \cdot t}{(b+h)} \qquad G = \frac{E}{2(1+\nu)} \tag{26}$$

Finally, the shear stresses at the top surface of the beam is given by

$$\sigma_{xy} = \frac{T}{2 \cdot b \cdot h \cdot t} \cdot [\tanh(\lambda L)\sinh(\lambda x) - \cosh(\lambda x) + 1] \tag{27}$$

According to Rice [33], for a two-dimensional mode II surface crack, the stress-intensity factor K_{II} due to internal stresses can be computed using the Green's function approach (Lawn [34]) as

$$K_{\mathrm{II}}|_{L,R} = \int_{-a}^{a} \sigma_{xy} G_{L,R}(x,a)\,\mathrm{d}x = \frac{1}{\sqrt{\pi a}} \int_{-a}^{a} \sigma_{xy} \sqrt{\frac{a \mp x}{a \pm x}}\,\mathrm{d}x \tag{28}$$

where $G(x,a)$ is the Green's function depending only on the geometry of the crack component configuration, and the subscripts L and R stand for the left and right crack tip of the crack (see Fig. 7), respectively. The shear stress σ_{xy} is almost constant along the domain where the crack is inserted (see Fig. 8). We can rewrite Eq. (28) in the form

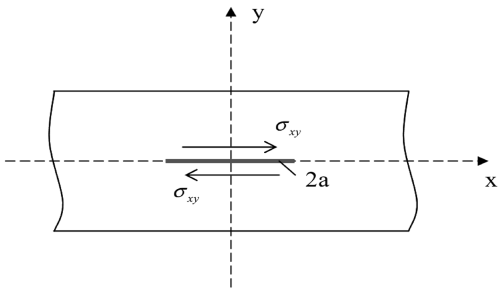

Fig. 7 Schematic model geometry.

$$K_{\mathrm{II}}|_{L,R} = \frac{1}{\sqrt{\pi a}} \int_0^a \sigma_{xy} \left(\sqrt{\frac{a-x}{a+x}} + \sqrt{\frac{a+x}{a-x}} \right) \mathrm{d}x \tag{29}$$

The mode II stress-intensity factor can be calculated as

$$K_{\mathrm{II}} = \frac{2a}{\sqrt{\pi a}} \int_0^a \frac{\sigma_{xy}}{\sqrt{a^2 - x^2}}\,\mathrm{d}x \tag{30}$$

Moving the x-y-z coordinate system to the center of the crack, and substituting Eq. (27) into Eq. (30), we obtain

$$K_{\mathrm{II}} = \frac{1}{\sqrt{\pi a}} \cdot \frac{T \cdot a}{b \cdot h \cdot t} \cdot \int_0^a \frac{1}{\sqrt{a^2 - x^2}} \times \left\{ \tanh(\lambda L)\sinh\left[\lambda\left(x + \frac{L}{2}\right)\right] - \cosh\left[\lambda\left(x + \frac{L}{2}\right)\right] + 1 \right\} \mathrm{d}x \tag{31}$$

or

$$K_{\mathrm{II}} = \frac{1}{\sqrt{\pi a}} \cdot \frac{T \cdot a}{b \cdot h \cdot t} \cdot \int_0^a \frac{1}{\sqrt{a^2 - x^2}} \times \left\{ -\frac{\cosh(\frac{\lambda L}{2})\cosh(\lambda x) - \sinh(\lambda x)\sinh(\frac{\lambda L}{2})}{\cosh(\lambda L)} + 1 \right\} \mathrm{d}x \tag{32}$$

Computation of the integrals in Eq. (32) will lead to the Bessel functions of the first kind. To compute the integral in Eq. (32), we need to compute the following integrals.

The first term in Eq. (32) can be written as

$$I_1 = \int_0^a \frac{\cosh(\lambda x)}{\sqrt{a^2 - x^2}}\,\mathrm{d}x \tag{33}$$

we use the following transformation ($x = a\sin(\theta)$, $\theta \in [0, (\pi/2)]$, and $\mathrm{d}x = a\cos(\theta)\,\mathrm{d}\theta$) to simplify Eq. (33) as

$$I_1 = \int_0^{\pi/2} \cosh[\lambda a \sin(\theta)]\,\mathrm{d}\theta \tag{34}$$

We can express the function cosh(.) as a Taylor series, and then I_1 can be rewritten in the form

$$I_1 = \int_0^{\pi/2} \cosh[\lambda a \sin(\theta)]\,\mathrm{d}\theta = \int_0^{\pi/2} \left[\sum_{n=1}^{\infty} \frac{(\lambda a)^{2n}}{(2n)!} \cdot \sin^{2n}(\theta)\,\mathrm{d}\theta + 1 \right] \mathrm{d}\theta \tag{35}$$

We have

$$\int_0^{\pi/2} \sin^{2n}(\theta)\,\mathrm{d}\theta = \frac{1, 3, 5, \ldots, (2n-1)}{2, 4, 6, \ldots, 2n} \cdot \frac{\pi}{2} \tag{36}$$

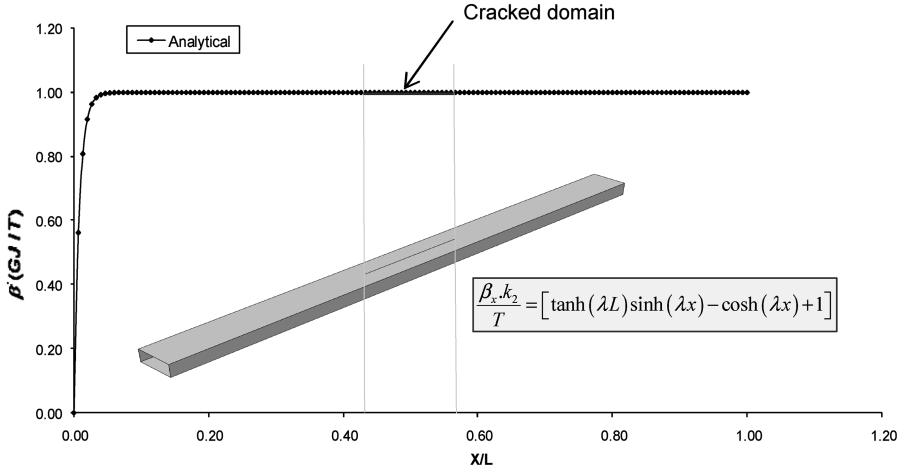

Fig. 8 Variation of the twist angle along the beam span.

After some algebraic operations, we finally obtain Eq. (33) in the form

$$I_1 = \sum_{n=1}^{\infty} \frac{(\lambda a)^{2n}}{2^{2n} \cdot (n!)^2} \frac{\pi}{2} + \frac{\pi}{2} \tag{37}$$

The second term in Eq. (32) can be written as

$$I_2 = \int_0^a \frac{\sinh(\lambda x)}{\sqrt{a^2 - x^2}}\, \mathrm{d}x \tag{38}$$

Similarly to the computation of the above integral, we can obtain

$$I_2 = \sum_{n=1}^{\infty} \frac{(\lambda a)^{2n+1}}{((2n+1)!)^2} + \lambda a \tag{39}$$

The third term in Eq. (32) can be easily computed, as shown above.

We use the transformation $x = a\sin(\theta)$, $\theta \in [0, (\pi/2)]$, and $\mathrm{d}x = a\cos(\theta)\,\mathrm{d}\theta$; therefore,

$$I_3 = \int_0^a \frac{1}{\sqrt{a^2 - x^2}}\, \mathrm{d}x = \frac{\pi}{2} \tag{40}$$

Substituting Eqs. (38–40) into Eq. (32), we obtain Eq. (32) in the form

$$K_{\mathrm{II}} = \frac{T}{2 \cdot b \cdot h \cdot t} \sqrt{\pi a} \left[\frac{-I_1 \cdot \cosh(\frac{\lambda L}{2}) + I_2 \cdot \sinh(\frac{\lambda L}{2})}{\cosh(\lambda L)} \cdot \frac{2}{\pi} + 1 \right] \tag{41}$$

where

$$I_1 = \sum_{n=1}^{\infty} \frac{(\lambda a)^{2n}}{2^{2n} \cdot (n!)^2} \frac{\pi}{2} + \frac{\pi}{2} \qquad I_2 = \sum_{n=1}^{\infty} \frac{(\lambda a)^{2n+1}}{((2n+1)!)^2} + \lambda a$$

Expression (41) can be used for small cracks and it is accurate within 2% in comparison with shell finite element models for crack lengths $(a/b) \le 0.125$ (or $l_{\mathrm{crack}} \le 0.25b$). This can be seen in numerical examples in the next section. For small cracks, the beam behaves almost as a closed rectangular thin-walled beam. For the rectangular cross sections, k_1 and k_2 in Eq. (11) can be computed as

$$k_1 = \frac{t \cdot (b \cdot h)^2 \cdot (b-h)^2}{24 \cdot (b+h)} \cdot E \qquad k_2 = \frac{2 \cdot (b \cdot h)^2 \cdot t}{(b+h)} \cdot \frac{E}{2(1+\nu)} \tag{42}$$

And therefore λ in Eq. (18) can be written in the form

$$\lambda = \sqrt{\frac{k_2}{k_1}} = \frac{2}{|b-h|} \sqrt{\frac{6}{1+\nu}} \tag{43}$$

An observation for thin-walled structures as defined in Eq. (1) has the value of λL to be very large:

$$\lambda L = \frac{2}{|b-h|} \sqrt{\frac{6}{1+\nu}} . L = \frac{2}{\frac{|b-h|}{L}} \sqrt{\frac{6}{1+\nu}} \succ \frac{2}{\frac{\max(b,h)}{L}} \sqrt{\frac{6}{1+\nu}}$$
$$\succ 20 \sqrt{\frac{6}{1+\nu}} \succ 20 \sqrt{\frac{6}{1+0.5}} = 40 \tag{44}$$

This leads to

$$\tanh(\lambda L) = \frac{e^{2\lambda L} - 1}{e^{2\lambda L} + 1} \simeq 1 \qquad \sinh(\lambda L) \simeq \cosh(\lambda L) \tag{45}$$

It means that the first term in the bracket in Eqs. (31) and (32) is very small and can be neglected. For example, $b = 0.4$, $h = 0.2$, and $L = 6$; λ is approximated equally as 21.24 and $\lambda L = 127.44$. The derivative of the twist angle of the beam is almost constant along the crack length $2a$. The term in the bracket of Eqs. (24) and (41) is approximately 1 (see Fig. 8). Obviously, as $b = h$, $\lambda \to \infty$, the twist angle in Eq. (17) is $\beta = (T/k_2)x$, and when the beam becomes the square cross-sectional thin-walled beams of constant thickness, with no significant primary warping.

Therefore, the shear stresses along the cracked domain can be approximated as $\sigma_{xy} = T/(2 \cdot b \cdot h \cdot t)$. Expression (41) can be approximated as

$$K_{\mathrm{II}} = \frac{T}{2 \cdot b \cdot h \cdot t} \sqrt{\pi a} \tag{46}$$

where

$$\frac{a}{b} \le 0.125 \quad (\text{or } l_{\mathrm{crack}} \le 0.25b)$$

Figure 9 shows the plot of the analytical solution, as shown in Eq. (41) and the simplified solution is shown in Eq. (46).

Since the beam has a long crack, the behavior of the beam at the cracked domain is more complex (see Fig. 10). A very long crack along the beam span can make the beam locally behave like an open cross section at the cracked domain with two clamped edges at the two crack tips; this will result in the deflection and rotation of the crack edges due to the torsional loading (see Fig. 10). Therefore, k_2, k_1, and λ are not exact, as shown in Eqs. (42) and (43) respectively. The twist angle varies along the beam span, and the first term in the bracket of Eq. (41) is not negligible.

To take into account the complex behavior of the thin-walled beams with a long crack along the beam span under the torsional loading (which leads to the deflection and rotation of the crack edges), we introduce a correction factor. The correction factor is based on the previous work of Folias [12] for estimating the stress-intensity factor of a longitudinal crack in a pressured cylindrical shell (Folias [12] and Janssen et al. [13]) and the empirical equations of Newman and Raju [10,11]. The correction factor for long cracks in our problem is derived based on a calibration using shell finite element calculations and is given as

$$C_f = \sqrt{1 + 2.52\frac{a^2}{b^2} - 1.2089\frac{a^4}{b^4}} \tag{47}$$

Our method is the same as the one that was used by Dunn [20]. Expression (46) for the mode II stress-intensity factor of thin-walled beams with a longitudinal crack can be written in the form

$$K_{\mathrm{II}} = \frac{T}{2 \cdot b \cdot h \cdot t} \cdot \sqrt{\pi a} \cdot C_f$$
$$= \frac{T}{2 \cdot b \cdot h \cdot t} \cdot \sqrt{\pi a} \cdot \sqrt{1 + 2.52\frac{a^2}{b^2} - 1.2089\frac{a^4}{b^4}} \tag{48}$$

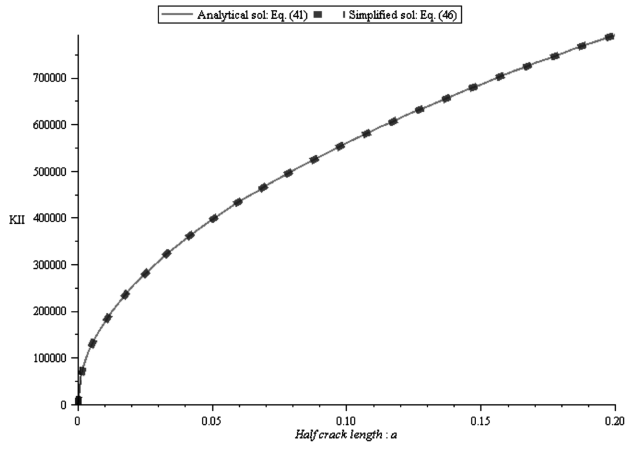

Fig. 9 Comparison of analytical solution in Eq. (41) and simplified solution in Eq. (46) for the thin-walled beam ($h = 0.2$, $b = 0.4$, $t = 0.01$, and $L = 6$).

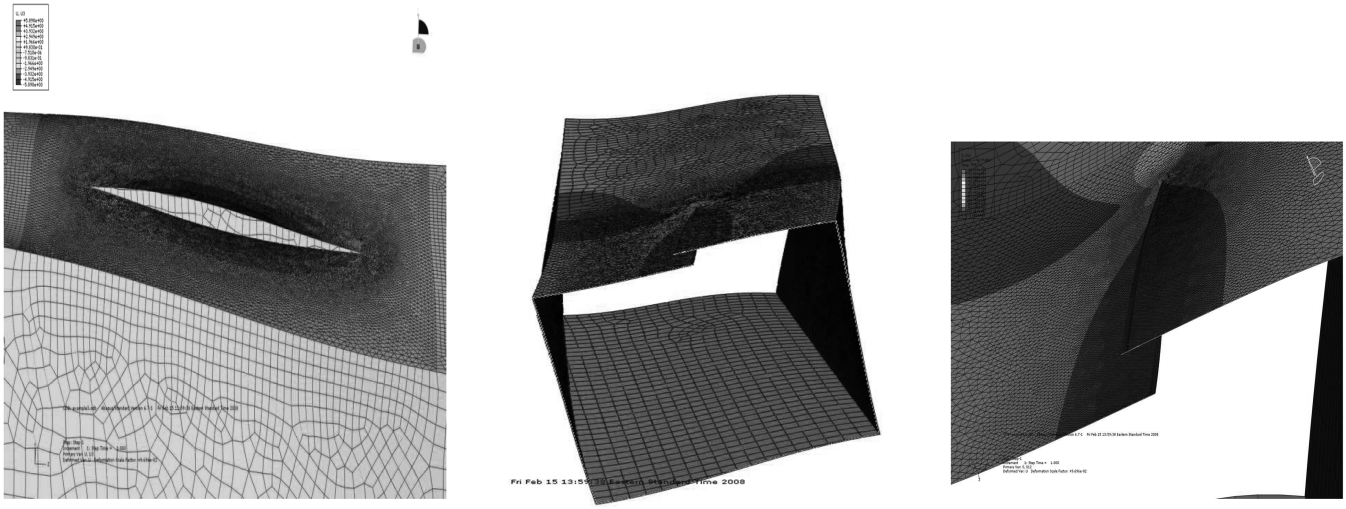

Fig. 10 Magnified view of the cracked domain of a cracked thin-walled beam with a long crack under a tip torque.

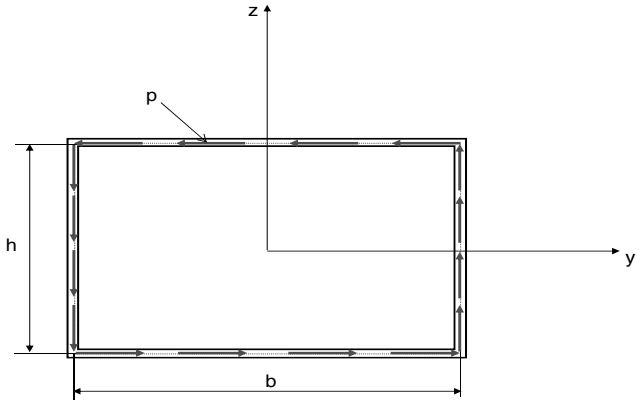

Fig. 11 Torsional loading applied $T = 10,000$ at the beam's tip by using shell edge load $p = 62500$.

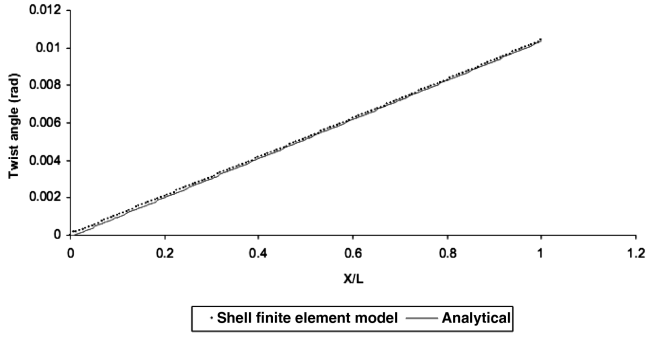

Fig. 12 Comparison of twist angle for closed-cross-section thin-walled beams.

This expression for the mode II stress-intensity factor is accurate within 3% in comparison to the results obtained from finite element models for any crack length $(a/b) \leq 1$ (or $l_{\text{crack}} \leq 2b$); we can see the numerical validation in the next section. Note that as $a/b \to 0$, then $C_f \to 1$, and therefore Eq. (48) returns to Eq. (46). As the crack length $a/b \leq 0.125$, the stress-intensity factor can be computed using Eq. (46) or Eq. (48), as the differences in the two formulas are very small.

In summary, the mode II stress-intensity factor for thin-walled beams with a longitudinal crack under the torsional loading can be computed as

$$K_{\text{II}} = \frac{T\sqrt{\pi a}}{2 \cdot b \cdot h \cdot t} \cdot \sqrt{1 + 2.52\frac{a^2}{b^2} - 1.2089\frac{a^4}{b^4}} \tag{49}$$

for any crack length with $(a/b) \leq 1$ (or $l_{\text{crack}} \leq 2b$.

III. Numerical Validation

A. Closed Cross Section of Thin-Walled Beams

We consider a closed cross section of thin-walled beam made of aluminum Al 7050-T7451 and it is clamped at $x = 0$. The beam has the following dimensions in a consistent set of units: length $L = 6$, width $b = 0.4$, depth $h = 0.2$, wall thickness $t_v = t_h = 0.01$, and torsion at its tip $T = 10,000$. The torsional loading is applied at the tip of the beam using shell edge loads $p = 62,500$, as shown in Fig. 11.

The problem is modeled by shell finite elements using ABAQUS; the results obtained from finite element (FE) model are compared with the analytical solutions in Eqs. (5) and (17). The results of the twist angle along the beam span from analytical solutions and shell finite element model in Fig. 12 are in very good agreement, and the difference between analytical solutions and shell FE models obtained

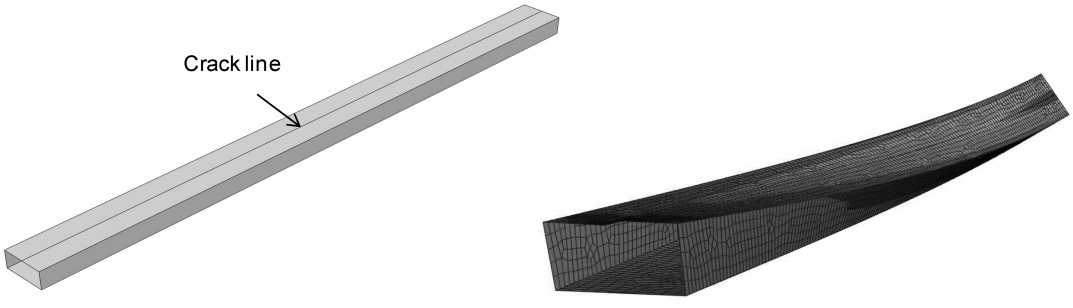

Fig. 13 Crack line description and shell finite element model for open-cross-section beams.

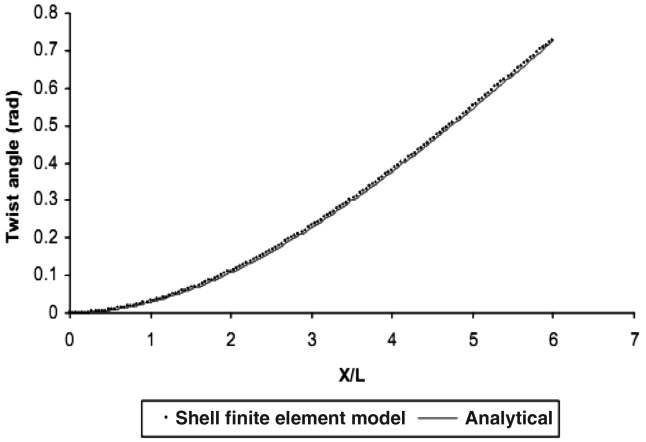

Fig. 14 Comparison of twist angle along the beam span for open-cross-section thin-walled beam.

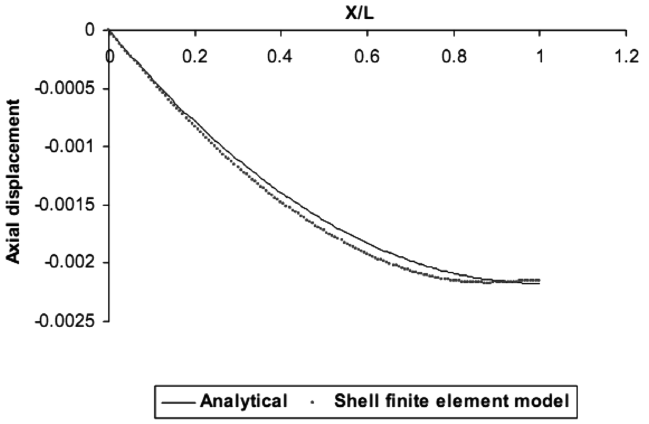

Fig. 15 Comparison of axial displacement along the beam span at $y = 0.2$ and $z = 0.1$.

is about 1.5%. Note that the axial displacement obtained along the central line of the beam under the pure torsion is almost zero.

B. Open Cross Section of Thin-Walled Beams

We consider a cross section of thin-walled beam with a crack along the whole length of the beam span, and thus it is considered to be an open-beam cross section (see Figs. 4 and 13). The beam is made of aluminum Al 7050-T7451 and has the same dimensions as the above closed-beam cross section in a consistent set of units. A tip torque $T = 10,000$ is applied, as shown in Fig. 11.

For a cracked cross section (see Fig. 4), the stiffness coefficients k_1 and k_2 are computed from Eq. (11) as

$$k_1 = \frac{E}{24}\left[\frac{tb^2h^2(10b^2 + 34bh + 3h^2)}{3h + b}\right]$$
$$k_2 = \frac{E}{12(1+\nu)}t^3(b + h) \tag{50}$$

Analytical solutions from Eqs. (5) and (17) are compared with those obtained from the shell finite element model using ABAQUS. Figures 14 and 15 show the comparison of twist angles and axial displacements between analytical solution and shell finite element model. The results are in very good agreement, and the maximum difference obtained in the case is about 0.5%. We can see that the axial displacement exhibits the warping deformation in Fig. 15, and the slope of the axial displacement for both analytical and finite element models are equal to zero at the tip of beam, which means that the second derivative of the twist angle at the tip of the beam is zero, as presented in Eq. (16).

C. Mode II Stress-Intensity Factor of Cracked Thin-Walled Beams

We consider a thin-walled beam, as shown in Fig. 6. The beam originally has a uniform rectangular closed cross section. An initial crack along the span of the beam is introduced with the crack length $2a = 0.02$. A tip torque $T = 1600\,(p = 10,000)$ is applied, as shown in Fig. 11. We take examples of different beam sizes and different values of thickness in a consistent set of units (see Fig. 16) to verify the expression for mode II stress-intensity factor given in Eq. (49).

The cracked thin-walled beam is modeled in ABAQUS using shell finite elements. To get the accurate stress-intensity factor, we need to have very fine mesh at the crack tips. In our problem, we use a rectangular box around the crack, the box has dimensions $(2a + 0.04, 0.02)$, where a is half of the crack length and the mesh size in the rectangular box is 0.0007. We set up 25 contours around the crack tip to get the value of stress-intensity factors converged. We also have other boxes around the rectangular box to ensure a smooth transition between the zone with very fine mesh and the other zones outside this box, where we use coarse mesh (see Fig. 17) to reduce the computational cost. The computational cost for solving fracture problems is normally very expensive and depends very much on the users' experience, and we need high-performance computers to model these problems. In our case, the CPU time for modeling a thin-walled beam with a longitudinal crack is 36 s on CPU Q 6850, 2.99 GHz, 3.25 GB RAM, and the wall-clock time for building the cracked thin-walled beam model is about 1.5 h.

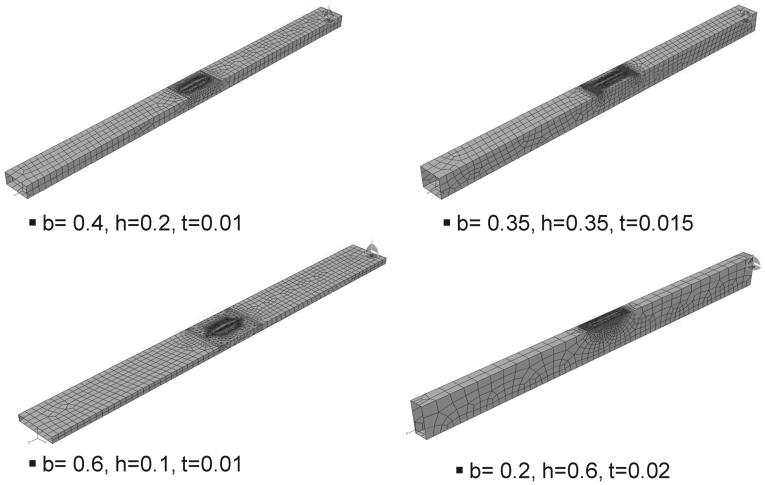

Fig. 16 Cracked thin-walled beam with different sizes used for numerical validation.

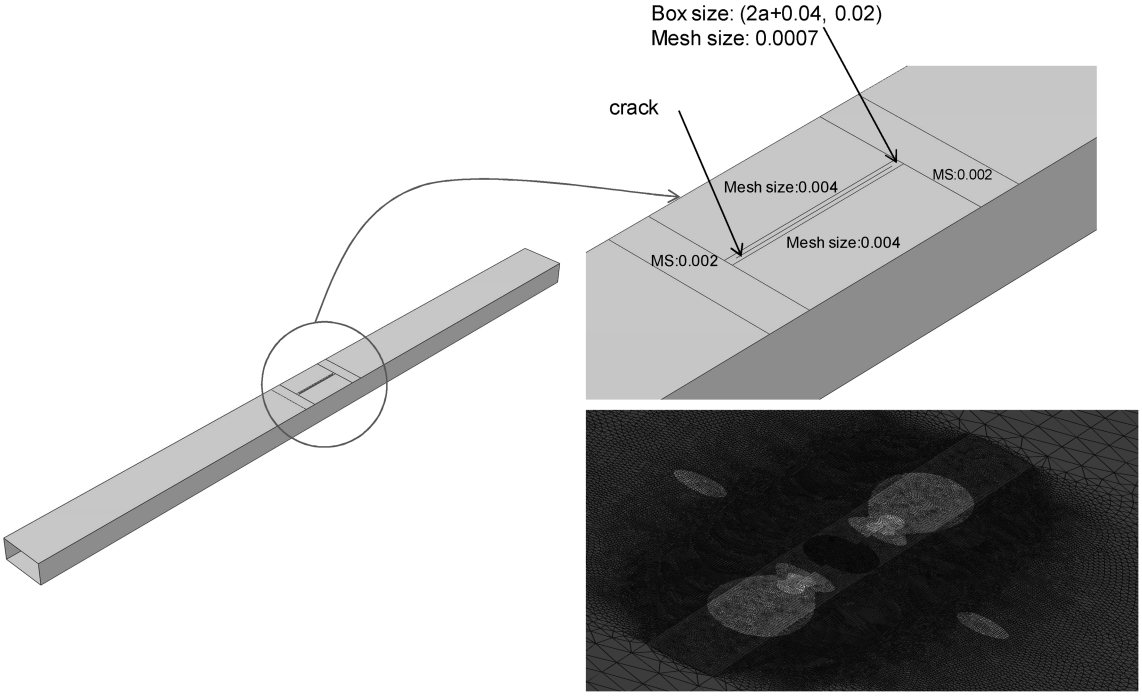

Fig. 17 Finite element mesh around the cracked domain.

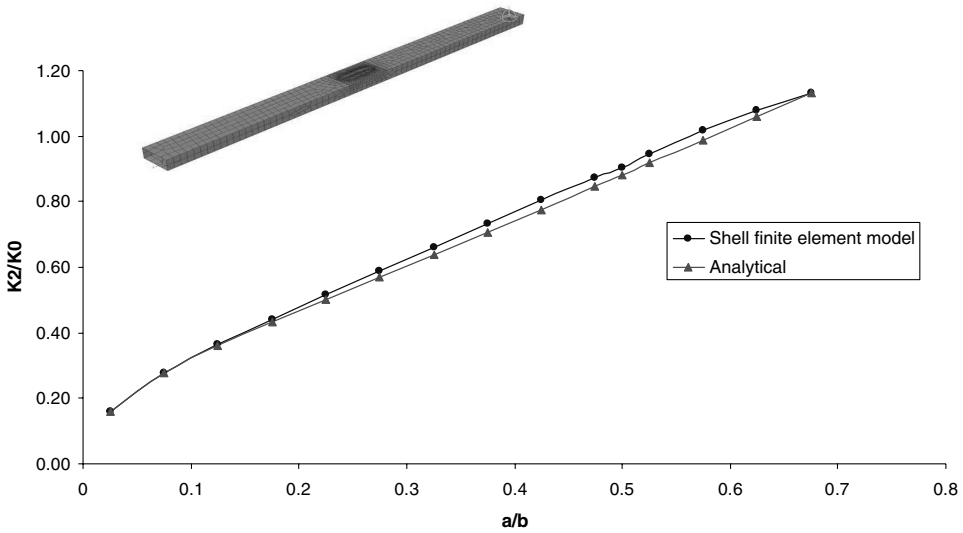

Fig. 18 Comparison of the results for mode II stress-intensity factor for the beam using the detailed FE modeling and the analytical solution ($b = 0.4$, $h = 0.2$, and $t = 0.01$).

Figures 18–21 show the comparison of the normalized mode II stress-intensity factor K_{II} between the analytical expression in Eq. (49) and that obtained from shell finite element model in ABAQUS for the different beam sizes (see Fig. 17), where a is half of the crack length, b is the width of the beam, h is the height of the beam, t is the thickness of the beam, and

$$k_o = \frac{T}{2 \cdot h \cdot b \cdot t} \sqrt{\pi b}$$

From Figs. 18–21, we realize that the mode II stress-intensity factor, computed using Eq. (49), matches very well with that obtained from the shell FE model. The maximum difference between the shell FE model and the analytical solution obtained in this case is 2.5% for the beam size $b = 0.4$, $h = 0.2$, and $t = 0.01$ in Fig. 18. Similarly, the difference between shell FE model and the analytical solution obtained for the beam size $b = 0.35$, $h = 0.35$, and $t = 0.015$ is 1.5% in Fig. 19; it is 1.8% for the beam size $b = 0.2$, $h = 0.6$, and $t = 0.02$ in Fig. 20; and it is 2% for the beam size $b = 0.6$, $h = 0.1$, and $t = 0.01$ in Fig. 21.

IV. Conclusions

Thin-walled structures are widely used in engineering, and the understanding of the behavior under torsion is very important. Existence of defects and cracks in such beams is inevitable and may cause unexpected failure. The current paper deals with the analysis of closed and open thin-walled beams under torsion, in the presence of a longitudinal crack. In this study, analytical solutions for twist angles, stresses, and strains have been derived using the principle of virtual work. The analysis takes into account nonclassical effects such as primary and secondary torsional warping. A closed-form expression of the mode II stress-intensity factor for the rectangular thin-walled beams with a longitudinal crack is found for the first time; the

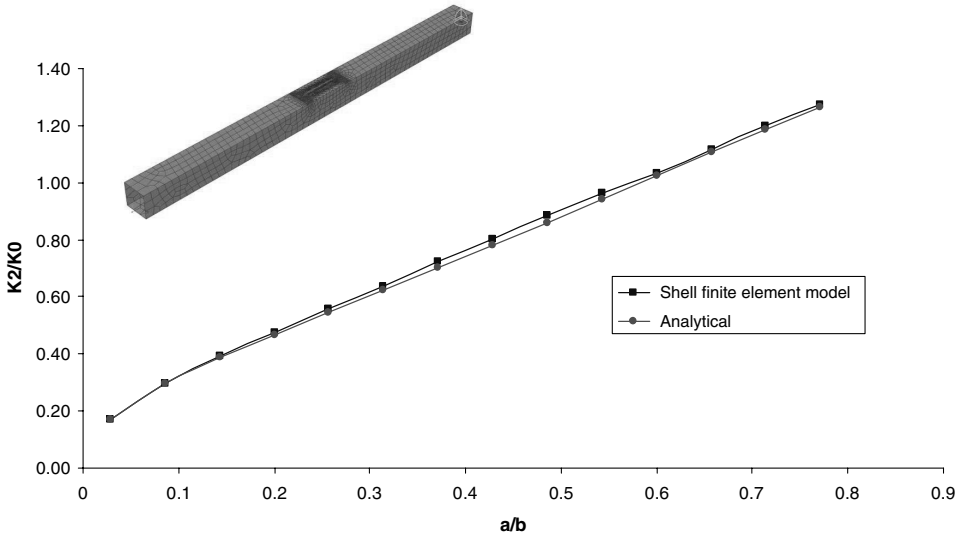

Fig. 19 Comparison of the results for mode II stress-intensity factor for the beam using the detailed FE modeling and the analytical solution ($b = 0.35$, $h = 0.35$, and $t = 0.015$).

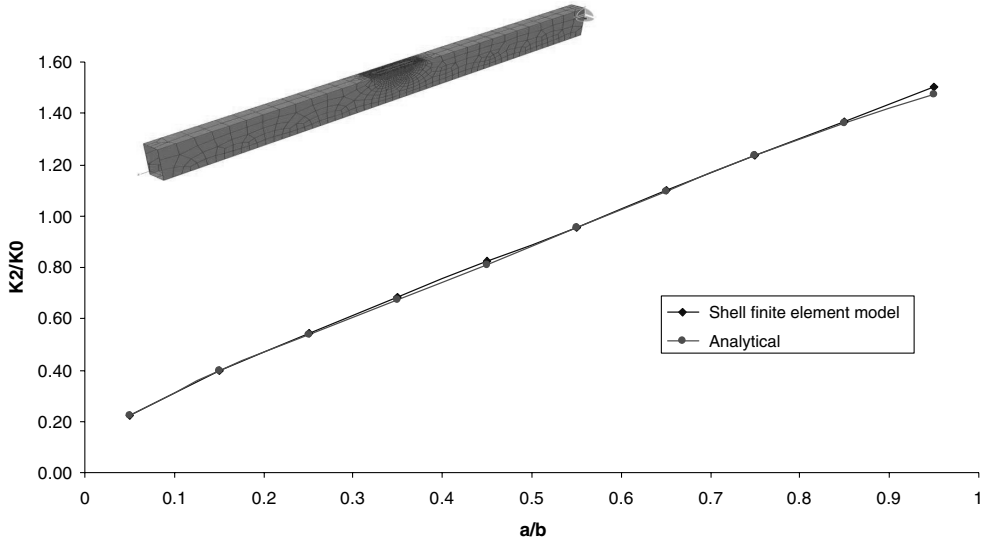

Fig. 20 Comparison of the results for mode II stress-intensity factor for the beam using the detailed FE modeling and the analytical solution ($b = 0.2$, $h = 0.6$, and $t = 0.02$).

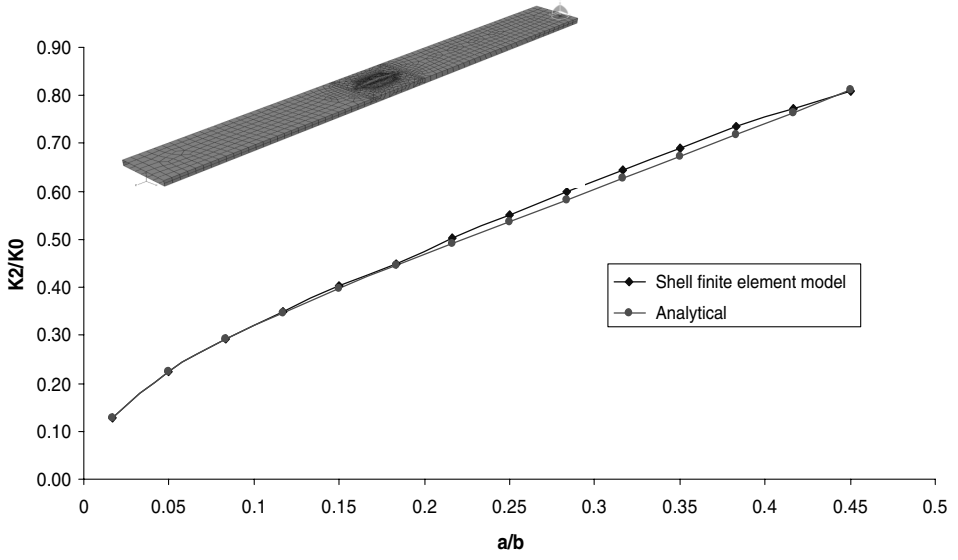

Fig. 21 Comparison of the results for mode II stress-intensity factor for the beam using the detailed FE modeling and the analytical solution ($b = 0.6$, $h = 0.1$, and $t = 0.01$).

expression is very easy and convenient for use in practical problems. The analytical solutions are verified with those obtained from shell finite element models using ABAQUS. The results in the current paper are the first step to compute critical loadings for thin-walled beams in the presence of cracks and to better understand the local and global behavior of the cracked thin-walled beams under torsion.

Appendix: Procedure to Determine Warping Functions

To determine the warping function, we follow the procedure described by Murray [28]. A brief description of this procedure follows.

Step 1. Locate the origin of the coordinate system $\bar{y}o\bar{z}$, the pole P, and the starting point C at convenient points (see Fig. 4). We find all the section properties F, $\bar{\psi}$, and $F_{\bar{\psi}p}$ using this coordinate system as follows:

Area of cross section,

$$F = \int_A \mathrm{d}A$$

First moment of area about the $\bar{y}$ axis,

$$F_{\bar{z}} = \int_A \bar{z}(s)\,\mathrm{d}A$$

First moment of area about the $\bar{z}$ axis,

$$F_{\bar{y}} = \int_A \bar{y}(s)\,\mathrm{d}A$$

First moment area about pole P,

$$F_{\bar{\psi}} = \int_A \bar{\psi}_p(s)\,\mathrm{d}A$$

Second moment of area of the cross section about the $\bar{y}$ axis,

$$F_{\bar{z}\bar{z}} = \int_A \bar{z}^2(s)\,\mathrm{d}A$$

Second moment of area of the cross section about the $\bar{z}$ axis,

$$F_{\bar{y}\bar{y}} = \int_A \bar{y}^2(s)\,\mathrm{d}A$$

Product moment of area of the cross section about the $\bar{x}, \bar{y}, \bar{z}$ coordinate system,

$$F_{\bar{z}\bar{y}} = \int_A \bar{z}(s)\bar{y}(s)\,\mathrm{d}A$$

Sectorial product of area,

$$F_{\bar{\psi}\bar{z}} = \int_A \bar{\psi}_P(s)\bar{z}(s)\,\mathrm{d}A$$

Sectorial product of area,

$$F_{\bar{\psi}\bar{y}} = \int_A \bar{\psi}_P(s)\bar{y}(s)\,\mathrm{d}A$$

Warping constant with pole P,

$$F_{\bar{\psi}\bar{\psi}} = \int_A \bar{\psi}_p^2(s)\,\mathrm{d}A$$

Step 2. Calculate the position of the centroid S as

$$\bar{z}_s = \int_A \frac{\bar{z}\,\mathrm{d}A}{F} \qquad \bar{y}_s = \int_A \frac{\bar{y}\,\mathrm{d}A}{F}$$

By a parallel shift of axes, move the origin to S, calling the $\tilde{x}$, $\tilde{y}$, and $\tilde{z}$. This transformation does not affect the warping function, since the warping function is determined using the sectorial area that remains unchanged for a given pole P and the starting point C. The new reference coordinate system is now $\tilde{y}s\tilde{z}$.

Step 3. To obtain $\tilde{\psi}_P$, subtract the value $\bar{\psi}_o$ from $\bar{\psi}_P(s)$, where

$$\bar{\psi}_o = \frac{F_{\bar{\psi}}}{F}$$

This step is to ensure that

$$\int_A \tilde{\psi}_p(s)\,\mathrm{d}A = 0$$

Calculate the section properties F in the coordinate system $\tilde{y}s\tilde{z}$ as

$$F_{\tilde{z}\tilde{\psi}} = F_{\bar{z}\bar{\psi}} - \frac{F_{\bar{z}}F_{\bar{\psi}}}{F}$$

$$F_{\tilde{y}\tilde{\psi}} = F_{\bar{y}\bar{\psi}} - \frac{F_{\bar{y}}F_{\bar{\psi}}}{F}$$

$$F_{\tilde{z}\tilde{z}} = F_{\bar{z}\bar{z}} - \frac{F_{\bar{z}}^2}{F}$$

$$F_{\tilde{y}\tilde{y}} = F_{\bar{y}\bar{y}} - \frac{F_{\bar{y}}^2}{F}$$

$$F_{\tilde{\psi}\tilde{\psi}} = F_{\bar{\psi}\bar{\psi}} - \frac{F_{\bar{\psi}}^2}{F}$$

Step 4. The axes $\tilde{z}$ and $\tilde{y}$ should be rotated into the direction of the principal axes x and y, the angle of rotation ψ being given by

$$\tan 2\psi = \frac{2F_{\tilde{z}\tilde{y}}}{-F_{\tilde{y}\tilde{y}} + F_{\tilde{z}\tilde{z}}}$$

and the coordinates of the shear center P^* are computed as

$$\tilde{z}_{P^*} - \tilde{z}_P = \frac{F_{\tilde{\psi}_P\tilde{y}}F_{\tilde{z}\tilde{z}} - F_{\tilde{\psi}_P\tilde{z}}F_{\tilde{z}\tilde{y}}}{F_{\tilde{z}\tilde{z}}F_{\tilde{y}\tilde{y}} - F_{\tilde{z}\tilde{y}}^2}$$

$$\tilde{y}_{P^*} - \tilde{y}_P = \frac{F_{\tilde{\omega}_P\tilde{y}}F_{\tilde{z}\tilde{y}} - F_{\tilde{\psi}_P\tilde{z}}F_{\tilde{y}\tilde{y}}}{F_{\tilde{z}\tilde{z}}F_{\tilde{y}\tilde{y}} - F_{\tilde{z}\tilde{y}}^2}$$

Step 5. Move the pole from P to P^* and transform $\tilde{\psi}_P(s)$ to the value $\psi_{P^*}(s)$ so that

$$\int_A \psi_{p^*}(s)\,\mathrm{d}A = 0$$

Thus, the warping function is finally achieved as follows:

$$\psi_{P^*}(s) = \tilde{\psi}_P(s) + (\tilde{y}_{P^*} - \tilde{y}_P)\tilde{z} - (\tilde{z}_{P^*} - \tilde{z}_P)\tilde{y}$$

Acknowledgments

This work was supported by the NASA Integrated Resilient Aircraft Control program (agreement no. NNX08AC49A) with T. Krishnamurthy (NASA Langley Research Center) as the technical monitor. The authors also appreciate the discussions with A. Ingraffea of Cornell University.

References

[1] Papangelis, J. P., and Hancock, G. J., "Computer Analysis of Thin-Walled Structural Members," *Computers and Structures*, Vol. 56, No. 1, 1995, pp. 157–176. doi:10.1016/0045-7949(94)00545-E

[2] Kapania, R. K., and Castel, F., "A Simple Element for Aeroelastic Analysis of Undamaged and Damaged Wings," *AIAA Journal*, Vol. 28, No. 2, 1990, pp. 329–337. doi:10.2514/3.10393

[3] Dimarogonas, A. D., "Vibration of Cracked Structures: A State of the Art Review," *Engineering Fracture Mechanics*, Vol. 55, No. 5, 1996, pp. 831–857. doi:10.1016/0013-7944(94)00175-8

[4] Ruotolo, R., and Surace, C., "Damage Assessment of Multiple Cracked Beams: Numerical Results and Experimental Validation," *Journal of Sound and Vibration*, Vol. 206, No. 4, 1997, pp. 567–588. doi:10.1006/jsvi.1997.1109

[5] Chondros, T. G., Dimarogonas, A. D., and Yao, J., "A Continuous Cracked Beam's Vibration Theory," *Journal of Sound and Vibration*, Vol. 215, No. 1, 1998, pp. 17–34. doi:10.1006/jsvi.1998.1640

[6] Song, O., Ha, T. W., and Librescu, L., "Dynamics of Anisotropic Composite Cantilevers Weakened by Multiple Transverse Open Cracks," *Engineering Fracture Mechanics*, Vol. 70, No. 1, 2003, pp. 105–123. doi:10.1016/S0013-7944(02)00022-X

[7] Wang, K., Inman, D. J., and Farrar, C. R., "Modeling and Analysis of a Cracked Composite Cantilever Beam Vibrating in Coupled Bending and Torsion," *Journal of Sound and Vibration*, Vol. 284, Nos. 1–2, 2005, pp. 23–49. doi:10.1016/j.jsv.2004.06.027

[8] Wang, K., and Inman, D. J., "Crack-Induced Effects on Aeroelasticity of an Unswept Composite Wing," *AIAA Journal*, Vol. 45, No. 3, 2007, pp. 542–551. doi:10.2514/1.21689

[9] Sih, G. C., *Mechanics of Fracture: Methods of Analysis and Solutions of Crack Problems*, Noordhoff, Leyden, The Netherlands, 1973.

[10] Newman, J. C., and Raju, I. S., "An Empirical Stress Intensity Factor Equation for the Surface Crack," *Engineering Fracture Mechanics*, Vol. 15, No. 1–2, 1981, pp. 185–192. doi:10.1016/0013-7944(81)90116-8

[11] Newman, J. C., and Raju, I. S., "Stress Intensity Factor Equations for Cracks in 3D Finite Bodies Subjected to Tension and Bending Loads," NASA TM 85793, 1984.

[12] Folias, E. S., "An Axial Crack in a Pressure Cylindrical Shell," *International Journal of Fracture*, Vol. 1, No. 2, 1965, pp. 104–113.

[13] Janssen, M., Zuidema, J., and Wanhill, R., *Fracture Mechanics*, 2nd ed., Spon Press, New York, 2004.

[14] Sanders, J. L., "Circumferential Through-Cracks in Cylindrical Shells Under Tension," *Journal of Applied Mechanics*, Vol. 49, No. 1, 1982, pp. 103–107. doi:10.1115/1.3161948

[15] Sanders, J. L., "Circumferential Through-Cracks in a Cylindrical Shells Under Combined Bending and Tension," *Journal of Applied Mechanics*, Vol. 50, No. 1, 1983, p. 221. doi:10.1115/1.3166999

[16] Herrmann, G., and Sosa, H., "On Bars with Cracks," *Engineering Fracture Mechanics*, Vol. 24, No. 6, 1986, pp. 889–894. doi:10.1016/0013-7944(86)90273-0

[17] Bazant, Z. P., "Justification and Improvement of Kienzler and Herrmann's Estimate of Stress Intensity Factors of Cracked Beam," *Engineering Fracture Mechanics*, Vol. 36, No. 3, 1990, pp. 523–525. doi:10.1016/0013-7944(90)90298-U

[18] Gao, H., and Herrmann, G., "On Estimates of Stress Intensity Factors for Cracked Beams and Pipes," *Engineering Fracture Mechanics*, Vol. 41, No. 5, 1992, pp. 695–706. doi:10.1016/0013-7944(92)90154-7doi:

[19] Muller, W. H., Herrmann, G., and Gao, H., "Elementary Strength Theory of Cracked Beams," *Theoretical and Applied Fracture Mechanics*, Vol. 18, No. 2, 1993, pp. 163–177. doi:10.1016/0167-8442(93)90042-A

[20] Dunn, M. L., Suwito, W., and Hunter, B., "Stress Intensity Factors for Cracked I-Beams," *Engineering Fracture Mechanics*, Vol. 57, No. 6, 1997, pp. 609–615. doi:10.1016/S0013-7944(97)00059-3

[21] Xie, Y. J., Xu, H., and Li, P. N., "Crack Mouth Widening Energy-Release Rate and Its Application," *Theoretical and Applied Fracture Mechanics*, Vol. 29, No. 3, 1998, pp. 195–203. doi:10.1016/S0167-8442(98)00030-5

[22] Xie, Y. J., "An Analytical Method on Circumferential Periodic Cracked Pipes and Shells," *International Journal of Solids and Structures*, Vol. 37, No. 37, 2000, pp. 5189–5201. doi:10.1016/S0020-7683(99)00206-1

[23] Xie, Y. J., Wang, X. H., and Lin, Y. C., "Stress Intensity Factors for Cracked Rectangular Cross-Section Thin-Walled Tubes," *Engineering Fracture Mechanics*, Vol. 71, No. 11, 2004, pp. 1501–1513. doi:10.1016/S0013-7944(03)00217-0

[24] Yang H. T. Y., Saigal, S., Masud, A., and Kapania, R. K., "A Survey of Recent Shell Finite Elements," *International Journal for Numerical Methods in Engineering*, Vol. 47, Nos. 1–3, 2000, pp. 101–127. doi:10.1002/(SICI)1097-0207(20000110/30)47:1/3<101::AID-NME763>3.0.CO;2-C

[25] Librescu, L., and Song, O., *Thin-Walled Composite Beams: Theory and Application*, Springer, Amsterdam, 2006.

[26] Todhunter, I., and Pearson, K., *A History of the Theory of Elasticity and of the Strength of Materials*, Dover, New York, 1960.

[27] Gjelsvik, A., *The Theory of Thin Walled Bars*, Wiley, New York, 1981.

[28] Murray, N. W., *Introduction to the Theory of Thin-Walled Structures*, Oxford Univ. Press, New York, 1984.

[29] Oden, J. T., and Ripperger, E. A., *Mechanics of Elastic Structures*, 2nd ed., Hemisphere, New York, 1981.

[30] Fatmi, R. E., "Non-Uniform Warping Including the Effects of Torsion and Shear Forces. Part 2: Analytical and Numerical Applications," *International Journal of Solids and Structures*, Vol. 44, Nos. 18–19, 2007, pp. 5930–5952. doi:10.1016/j.ijsolstr.2007.02.005

[31] Smith, E. C., and Chopra, I., "Formulation and Evaluation of an Analytical Model for Composite Box-Beams," *Journal of the American Helicopter Society*, Vol. 36, No. 3, 1991, pp. 23–35. doi:10.4050/JAHS.36.23

[32] Prokic, A., "Computer Program for Determination of Geometrical Properties of Thin-Walled Beams with Open-Closed Section," *Computers and Structures*, Vol. 74, No. 6, 2000, pp. 705–715. doi:10.1016/S0045-7949(99)00076-0

[33] Rice, J. R., "Mathematical Analysis in the Mechanics of Fracture," *Fracture: An Advanced Treatise*, edited by H. Liebowitz, Vol. 11, Academic Press, New York, 1968, pp. 214–223.

[34] Lawn, B. R., *Fracture of Brittle Solids*, 2nd ed., Cambridge Univ. Press, Cambridge, England, U.K., 1993.

F. Pai
Associate Editor